PERGAMON

International Journal of Solids and Structures 38 (2001) 8989–8998

INTERNATIONAL JOURNAL OF SOLIDS and STRUCTURES

www.elsevier.com/locate/ijsolstr

Compressive superelastic behavior of a NiTi shape memory alloy at strain rates of 0.001–750 s^{-1}

Weinong W. Chen [a,*], QiuPing Wu [a], Joseph H. Kang [b], Nancy A. Winfree [b]

[a] *Department of Aerospace and Mechanical Engineering, University of Arizona, P.O. Box 210119, 1130 N Mountain, Tucson, AZ 85721-0119, USA*

[b] *Dominca, 9813 Admiral Dewey Avenue, NE, Albuquerque, NM 87111, USA*

Received 13 February 2001

Abstract

The compressive stress–strain behavior of a NiTi shape memory alloy (Nitinol SE508) has been determined over strain rates of 10^{-3}–7.5×10^{2} s^{-1}. A hydraulically driven load frame (Material test system, MTS 810) was used to conduct the quasi-static experiments. A split Hopkinson pressure bar with a pulse shaping technique was used to perform valid dynamic tests. Experimental results show that, the plateau stress of the shape memory alloy (SMA) is strain-rate dependent. Under quasi-static deformation and low-amplitude impact loading, the stress–strain curve of the SMA forms a closed hysteresis loop, with the material returning to its original length upon unloading. At higher dynamic loads, there is initially a residual deformation upon unloading, but the material slowly recovers its length. Dynamic strain lags behind the associated dynamic stress in the SMA specimen.

Keywords: Shape memory alloy; High strain rate behavior; Dynamic hysteresis; Split Hopkinson pressure bar; Nitinol

1. Introduction

Reversible martensitic phase transformations provide a number of alloys, called shape memory alloys (SMA), with the capabilities of shape memory and superelastic deformation. The mechanical behavior of SMA and recent research in the field are reviewed by Birman (1997), James and Hane (2000), and Bhattacharya (2001). A SMA possesses an austenite phase at high temperature and a martensitic phase at low temperature. There is a range of transition temperature over which temperature-induced phase transformation occurs. An object that appears to be permanently deformed at low temperature will return to its original shape when heated above the transition range because the martensitic phase transforms back to austenite. Two-way shape memory is also possible where the alloy remembers its shapes at both low and

* Corresponding author. Tel.: +1-520-621-6114; fax: +1-520-621-8191.
E-mail address: weinong@u.arizona.edu (W.W. Chen).

0020-7683/01/$ - see front matter
PII: S0020-7683(01)00165-2

high temperatures (Wayman, 1993). A two-way SMA will change its shape back and forth as the temperature is changed across the phase transformation region back and forth.

In addition to the temperature-induced phase transformations, martensitic transformation can be induced by mechanical stress in a certain temperature range. The range starts just above the temperature-induced phase transformation region (typically marked by the austenite finish transformation temperature, A_f) and ends at a temperature above which stress-induced martensitic transformation is not possible anymore, M_d (Stoeckel and Yu, 1991; Wayman, 1993; Duerig and Pelton, 1994). The alloy is austenite in this temperature range when stress-free. When the applied stress exceeds a threshold level, the austenite crystal structure will transfer to a martensitic phase. This stress-induced martensite (SIM) can be deformed by detwinning, which requires much less energy then to deform the austenite by conventional metal deformation mechanisms. The detwinning in the martensitic phase can accumulate up to 10% strain, which can be recovered completely by the reverse transformations back to austenite when the applied stress is removed. This large but reversible deformation is named superelasticity, a distinct property of SMA's.

When the temperature is in the superelasticity range, $A_f < T < M_d$, the stress–strain curve of a SMA obtained under quasi-static loading conditions is as shown schematically in Fig. 1. The idealized curve contains two plateaus. The upper plateau corresponds to the loading portion where the austenite is transforming into martensite and detwinning occurs in the newly formed SIM. The lower plateau represents the stress–strain behavior of the SMA during the unloading process where the SIM is transforming back to austenite. This stress–strain curve indicates that, even though the mechanical behavior is termed superelastic because there is no permanent deformation upon unloading, part of the mechanical energy used to deform the alloy is lost during unloading. Therefore, the loading/unloading cycle on the SMA leaves no permanent deformation but dissipates energy. The volume density of the lost energy in a loading/unloading cycle can be computed from the area within the hysteresis loop on the stress–strain curve shown in Fig. 1. Such an energy loss over a loading/unloading cycle makes it possible for the SMA to be used both as load-bearing structural components and as short-term shock/vibration absorption devices. In fact, SMA's have been described as "quiet" alloys (Schetky and Perkins, 1978). In order to efficiently use the SMA's both as a

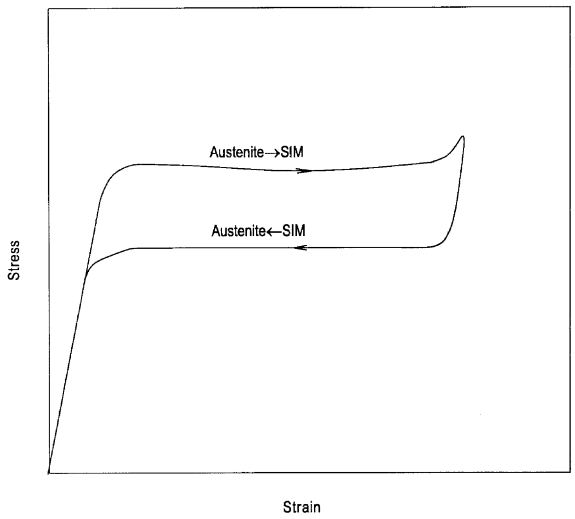

Fig. 1. A schematic quasi-static stress–strain curve of a SMA.

structural and energy-absorbing member in a variety of engineering applications, it is essential to quantitatively determine and understand the constitutive behavior of these alloys under dynamic loading conditions. However, such dynamic superelastic responses are not yet well characterized and well understood. In particular, reliable dynamic experimental methods are needed to obtain accurate dynamic mechanical responses of SMA's under high rates of loading.

In this paper, we present a modified split Hopkinson pressure bar (SHPB) technique to conduct valid dynamic compressive experiments on SMA. A valid SHPB experiment requires that the specimen undergo homogeneous deformation at a constant strain rate. Also, the stress in the specimen should be in dynamic equilibrium (Follansbee, 1985; Ravichandran and Subhash, 1994). To ensure that these conditions are satisfied when dynamically testing the SMA specimens using a SHPB, a pulse shaping technique was employed. The dynamic stress equilibrium process in the specimen was monitored using 1-wave/2-wave analysis on the non-dispersive waves created by the pulse-shaping technique. Experiments were conducted on Nitinol SE508 SMA in its superelastic temperature range. NiTi alloy is commonly referred to as Nitinol. The properties of NiTi alloys make them candidates to replace certain steels, titanium alloys, aluminum alloys and nickel-base superalloys in structures requiring energy-dissipating capacity. The following sections describe the experiments and present the results for the NiTi alloy.

2. Experimental setup and specimen preparation

To study the compressive behavior of the SMA, quasi-static experiments were conducted using a hydraulically driven materials test system (MTS 810) and a SHPB with pulse shaping was used to conduct dynamic compressive experiments. Both the quasi-static and the dynamic experiments were conducted at room temperature.

The SMA investigated in this research is NDC (Nitinol Devices & Components, Fremont, CA) SE508, nominally 55.8% nickel by weight and the balance titanium. The specified density is 6.5 g/cm^3, with an austenite finish transition temperature A_f of 5–18 °C and a melting point of 1310 °C. The temperature above which stress-induced martensitic transformation is no longer possible, M_d, for SE508 is approximately 150 °C. The temperature range for this alloy to exhibit superelasticity (the capability of returning to its original shape upon unloading after a substantial deformation) is 15–150 °C. Cylindrical specimens of 7.94-mm diameter by 8.10-mm long were machined at low speed on a lathe from as-drawn 7.94-mm diameter bar stock. Kool–Tool diluted in water was continuously sprayed on the contact area of the carbide tool and the bar to keep the temperature low in the NiTi alloy during machining. Specimens for the quasi-static experiments were 6.35-mm diameter by 12.7-mm long; the small diameter was used so that the maximum axial load was within the load cell capacity on the MTS machine. To give them their superelastic behavior the specimens machined from the as-drawn bar stock were then heat treated at 510 °C in a preheated furnace for 9 min and then water quenched in accordance with NDC's recommendations.

2.1. Quasi-static experiments

A hydraulically driven materials test system (MTS 810) was used to apply the axial compressive load in the quasi-static experiments. A specially built alignment/gripping device allowed the specimen to be loaded under boundary conditions nearly identical to those in the dynamic SHPB experiments except for the loading rate. An MTS load cell (model 1210AP-B) was used to measure the axial compressive load and an MTS extensometer (MTS-632.31E-24) to measure axial compressive strain. For greater accuracy over small strain ranges, a strain gage (Measurement Group, WK-06-031CF-350) was attached on each specimen.

2.2. Dynamic experiments

A SHPB with pulse shaping was used to conduct the dynamic compressive experiments. A schematic of the SHPB facility is shown in Fig. 2. The lengths of the VascoMax maraging steel bars used for the experiments were 1830, 762, and 305-mm for the incident, transmission, and striker bars, respectively, with a common diameter of 19-mm. The strain signals sensed by strain gages (Measurement Group, WK-06-250BF-10C) from the incident and transmission bars surfaces were recorded using a Tektronix TDS 420A digital storage oscilloscope through ADA400A differential amplifiers. For greater accuracy over small strain ranges, a strain gage (Measurement Group, WK-06-031CF-350) was also attached on each specimen during the dynamic experiments.

When the SHPB was used in a conventional configuration, that is, without a pulse shaper between the striker and the incident bar, the high-frequency oscillations in the incident pulse caused complications in the loading conditions in the specimen. The nature of stress-induced phase transformation makes the specimen sensitive to alternations of loading and unloading. Fig. 3 shows a typical oscilloscope record of a SMA undergoing dynamic loading by a conventional SHPB. There is no plateau in the reflected pulse shown in Fig. 3, which indicates that the specimen does not deform at a constant strain rate. The oscillations in the reflected pulse indicate that the specimen experiences a complicated deformation process. The point-wise dynamic material properties extracted by averaging the response over the specimen's volume cannot be expected to be accurate and reliable when the specimen is undergoing such a complicated deformation.

In order to obtain reliable dynamic material behavior from an SHPB experiment for the SMA, the rapid oscillations in the incident pulse must be avoided. Furthermore, efforts must be made to ensure that a dynamic equilibrium stress state is reached in the specimen during testing and to maintain a constant strain rate in the specimen. A homogeneously-deforming specimen under a dynamic equilibrium state of stress makes the volume-average of the specimen's behavior representative to the point-wise material properties. A constant strain rate eliminates the radial confinement due to inertia, thus maintaining a uniaxial stress state in the specimen. To eliminate the oscillations in the loading pulse and to ensure that the specimen deforms at a constant strain rate in dynamic equilibrium, a pulse shaper was placed on the impact end of the incident bar to control the shape of the loading pulse (Fig. 2). There are a variety of pulse-shaping devices. For example, Duffy et al. (1971) used a pulse shaper in the form of a concentric tube to smooth pulses generated by explosive loading in a torsional Hopkinson bar. Ravichandran and Chen (1991) and

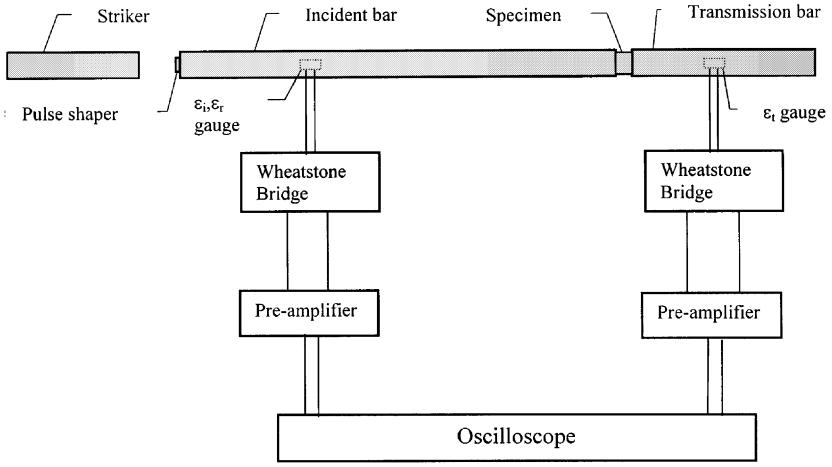

Fig. 2. A schematic of the modified SHPB.

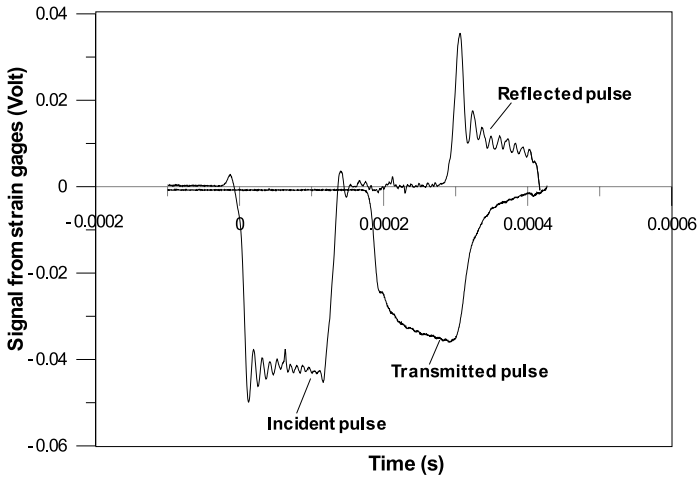

Fig. 3. Typical oscilloscope records of a conventional SHPB experiment on an SMA.

Nemat-Nasser et al. (1991) used copper pulse shapers to achieve ramp loading profiles when testing ceramics using SHPB. Togami et al. (1996) used a pulse shaper in a modified SHPB to control the loading pulse shape and to filter out high-frequency components in the incident pulse for accelerometer calibration up to 200,000 g. In the present research, annealed C11000 copper disks of various diameters and thicknesses were used. The diameter and the thickness necessary to control the strain rate in the SMA specimen at a desired and constant level was difficult to determine since the dynamic behavior of the SMA was unknown. Trial experiments were conducted to select a proper pulse shaper for each combination of desired strain rate and maximum strain.

3. Experiments and results

Quasi-static compressive experiments were conducted at room temperature to obtain data on the strain-rate effects on the mechanical response of this SMA alloy over a wide strain-rate range from quasi-static to dynamic. Fig. 4 presents the compressive stress–strain curves obtained under quasi-static loading conditions ($\dot{\varepsilon} = 10^{-3}$ s^{-1}) using a hydraulically driven materials test system (MTS 810). All the stress–strain curves shown in Fig. 4 were obtained from one NiTi specimen, which was loaded repeatedly to various peak axial strain levels, from 1.2% to 3.2%. As shown in Fig. 4, the shape of the quasi-static compressive stress–strain curves exhibits some of the fundamental characteristics of SMA. The initial elastic to plateau transition, that is, the transition from linearly elastic to superelastic, occurs at a stress of approximately 550 MPa. This transition indicates the stress-induced martensitic transformation inside the material. If the material is unloaded after being loaded into the superelastic region, the unloading portion of the stress–strain curve does not follow the loading portion, but follows a lower path back to the origin, which indicates the transformation of SIM back to austenite. All the stress–strain curves shown in Fig. 4 return to the origin upon unloading, i.e., all the hysteresis loops are completely closed.

A typical record on the oscilloscope for an SHPB experiment on the NiTi SMA with shaped pulses is shown in Fig. 5. The solid line is the transmitted pulse, which records the stress history in the specimen. The first pulse in the dashed line is the incident pulse, whereas the second is the reflected pulse. If the specimen's mechanical impedance (ρcA, where ρ is the mass density, c the bar wave velocity, and A cross-sectional area) is less than that of the bar, the incident and reflected pulses are always opposite in sign, as seen in Fig. 5.

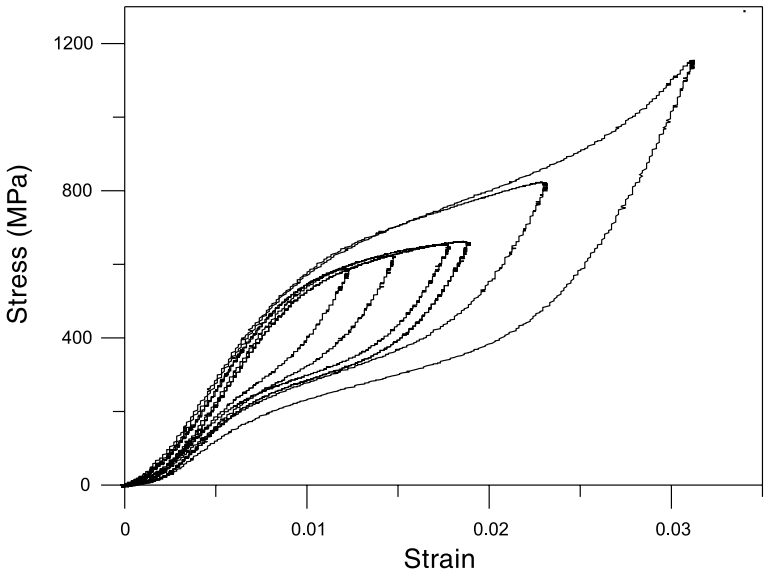

Fig. 4. Quasi-static compressive stress–strain curves of the NiTi SMA.

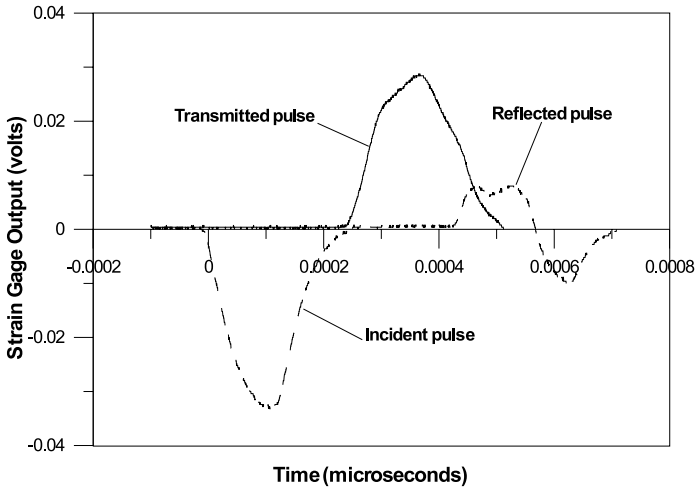

Fig. 5. Oscilloscope records of a pulse-shaped SHPB experiment on an SMA.

A comparison between the incident pulses of Figs. 3 and 5 indicates that the shape of the incident pulse in the pulse-shaped experiment shown in Fig. 5 is very different from that obtained in a conventional SHPB experiment (Fig. 3). The high-frequency oscillations on the incident pulse shown in Fig. 3 are completely eliminated after pulse shaping, as shown in Fig. 5. The nearly flat plateau on the reflected pulse shown in Fig. 5 indicates that the specimen deformed at a nearly constant strain rate during a pulse-shaped SHPB experiment on the NiTi SMA. The transmitted pulses were used to calculate stress history in the NiTi specimen according to conventional SHPB theory based on 1-D wave propagation theory (Kolsky, 1949;

Lindholm, 1964). The strain rate in the experiment was determined by the average magnitude of the plateau in the reflected pulse. The strain history was recorded by the strain gages mounted on the specimen surface.

In SHPB experiments, dynamic stress equilibrium in the specimen is a fundamental requirement for valid data processing because equilibrium is one of the basic assumptions upon which SHPB theory is built (Meyers, 1994). When dynamic equilibrium is impossible to reach, the constitutive behavior may be still found using a hybrid approach assisted by computer simulation if the form of the stress–strain relation is known. However, in the case of the NiTi SMA, the dynamic stress–strain relations are to be determined by the SHPB experiments. Dynamic equilibrium must be achieved such that the volume average of the stress–strain behavior over the entire specimen may be used as the pointwise material responses at a certain strain rate. It is therefore critical to ensure the dynamic equilibrium conditions are satisfied in order to obtain valid experimental results.

In our experiments, we checked stress equilibrium by comparing the transmitted signal (1-wave) with the difference between the incident and reflected signals (2-wave) (Gray et al., 1997; Wu and Gorham, 1997). This idealized method involves uncertainties in dispersion corrections and the distortion to the incident wave when reflected from a bar/specimen interface. However, the incident wave created by pulse shaping is nearly non-dispersive since there are no high-frequency components associated with the main loading pulse. Therefore, the results on stress equilibrium from 1-wave, 2-wave analysis are considered to be reliable. Fig. 6 shows the results of such an analysis on the stress pulses of Fig. 5. There are two nearly-overlapped curves shown in Fig. 6. One is the transmitted pulse profile (1-wave), and the other is the difference between the incident and the reflected pulses (2-wave). The 2-wave curve represents the axial force history on the face of the specimen that is in contact with the incident bar (Gray et al., 1997; Wu and Gorham, 1997). The 1-wave curve, which is used to calculate the stress history in SHPB data reduction, is the axial force history on the face of the SMA specimen that is in contact with the transmission bar during an experiment. Dynamic stress equilibrium in the specimen requires that the 1-wave and the 2-wave are the same over the duration of the SHPB experiment. Fig. 6 shows that, after careful pulse shaping, the 1-wave curve nearly overlaps the 2-wave curve, which indicates that dynamic equilibrium stress state in the specimen has been achieved. Furthermore, the amplitude of the reflected pulse is nearly constant as shown in Fig. 5, which indicates a

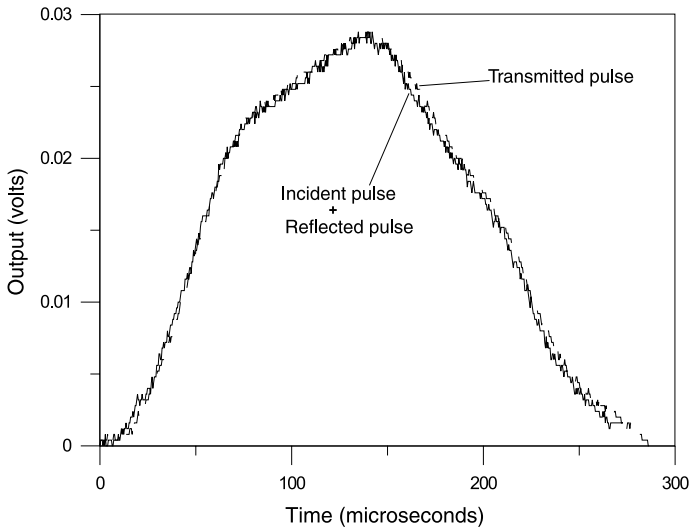

Fig. 6. Dynamic equilibrium analysis by 1-wave/2-wave method.

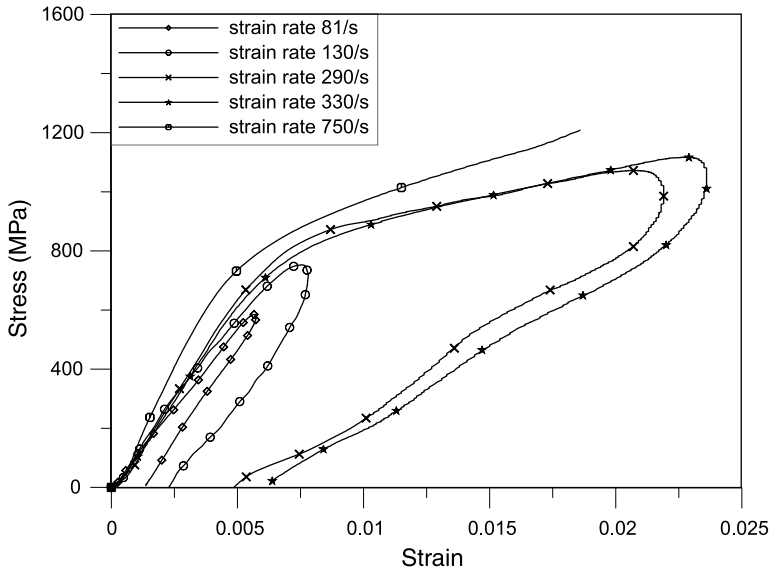

Fig. 7. Dynamic compressive stress–strain curves of the NiTi SMA.

constant strain rate over the duration of the experiment. Therefore the SHPB test recorded in Fig. 5 is a valid dynamic experiment. Such analysis was performed on every experiment presented here.

Fig. 7 summarizes the dynamic compressive stress–strain curves at strain rates from 81 to 750 s^{-1} for the Nitinol SE508 NiTi SMA. The experiments were performed at room temperature, which is between the austenite transformation finish temperature, A_f, and the terminal temperature for SIM, M_d, of the SMA. The stress–strain curves are plotted in the units of engineering stress and strain, which are nearly identical to true stress and strain curves, since the total deformation experienced by the specimens is small. As shown in Fig. 7, after a linearly elastic region, the stress–strain curves start to bend into a plateau-like region at a stress level of about 800 MPa. The stress–strain curve at the strain rate of 750 s^{-1} stopped at a strain of ~2% where the strain gage on the specimen failed. The transition stress is slightly higher when the strain rate is increased from 130 to 750 s^{-1}. However, the dynamic transition stress is ~45% higher than the quasi-static transition stress of ~550 MPa. Therefore, the transition stress between the linearly elastic region and the superelastic region is highly strain-rate dependent. When the strain rate is below 100 s^{-1}, the striker bar initial velocity had to be set at such a low level that the amplitude of the loading pulse was not large enough to load the specimen beyond its plateau stress level. Upon unloading, all the dynamic compressive stress–strain curves show hysteresis loops. For comparison, results from an SHPB experiment conducted on a 4340 steel specimen heat treated to Rc 45 under the same experimental conditions showed no hysteresis loop. Therefore, the loop is indeed a dynamic material property of this SMA. Furthermore, the loops do not close completely when the stress is reduced to zero. However, a post-test measurement of the specimen length with 0.001-mm resolution digital micrometer showed no measurable permanent or residual strain when the maximum strain in the specimen was below 1% during the dynamic experiment. When the total strain exceeded 2% under dynamic loading, residual strain could be measured immediately after the experiment. However, the residual strain then disappeared, i.e., the specimen recovered in as short as ~30 s to as long as 24 h at room temperature after the dynamic loading. Therefore, the material will recover completely, but not immediately.

To better understand the dynamic hysteresis behavior, typical stress and strain histories in the NiTi SMA specimen during a dynamic SHPB experiment are shown in Fig. 8. These histories are associated with

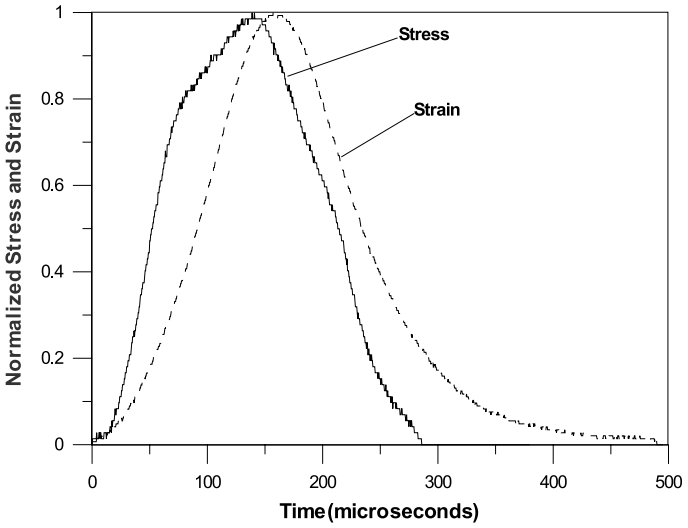

Fig. 8. Dynamic compressive stress and strain histories in the NiTi SMA.

the dynamic experiment conducted at a strain rate of 290 s^{-1} whose stress–strain curve is shown in Fig. 7. The units associated with the vertical axis have been normalized to clearly illustrate their amplitude variations with time: 1.0 corresponds to a stress of 1050 MPa and a strain of 2.15%. Fig. 8 clearly shows that the strain rises gradually from zero to its peak value at a nearly constant rate. However, the stress pulse rises fast initially, then rises rate at a slower rate above 0.8 normalized stress. This corresponds to the transition from linearly elastic to superelastic shown in Fig. 7. The peak of the strain pulse is ~17 μs behind the stress peak, i.e., the strain history reaches its peak 17 μs after the unloading begins. This type of behavior, namely a time shift, is a typical mechanical response for viscoelastic materials, but not commonly seen in engineering metals. However, the time shift is consistent with the residual deformation in the hysteresis behavior of Fig. 7. Further inspection of the stress and strain histories reveals that, at lower strain rate, e.g., 81 s^{-1}, there is no noticeable time shift behavior. As the strain rate increases to above 100 s^{-1}, the unloading portion of the strain history starts to lag behind the corresponding stress history. At even higher strain rates, strain lags behind stress during both loading and unloading as shown in Fig. 8.

4. Conclusions

A SHPB was employed, together with a pulse-shaping technique, to determine the dynamic compressive stress–strain behavior of a Nitinol SE508 SMA in its superelasticity phase. Dynamic stress equilibrium and constant strain rate conditions were checked for each experiment to ensure that the experiments were valid and the results accurate.

Experimental results show that the compressive stress–strain behavior of the SMA is dependent on strain rate. Under quasi-static loading conditions, the compressive stress–strain curves of the SMA exhibit closed hysteresis loops, with the specimens recovering completely upon unloading. Upon loading, there is a transition from a stiff behavior to a soft behavior at approximately 550 MPa. The material is initially stiff upon unloading but then softens at a stress level of ~300 MPa, and stiffens again as the stress approaches zero.

Under dynamic loading, the compressive stress–strain curves also show hysteresis loops, but they are open rather than closed. There is residual deformation of the specimens that disappears with time at room temperature, but it may take a few seconds to several hours before recovery is complete. Dynamic strain history lags behind the associated stress history in the specimen. The higher the strain rate, the more severe the lagging. There is a transition from a stiff to soft behavior upon loading, but it occurs at about 800 MPa, considerably higher than the transition stress for the quasi-static experiments. Upon unloading, there is no clear transition from stiff to soft behavior.

Acknowledgements

The authors wish to thank Dr. Bo Song and Mr. Zunping Liu for their assistance in the experimental work in this research project. This work was supported in part by the US Air Force Research Laboratory through the Small Business Innovation Research (SBIR) program under contract F08630-00-C-0044.

References

Bhattacharya, K., 2001. Theory of martensitic microstructure and the shape-memory effect. Shape Memory Alloys, in press.

Birman, V., 1997. Review of mechanics of shape memory alloy structures. Applied Mechanics Review 50, 629–645.

Duerig, T.W., Pelton, A.R., 1994. Ti–Ni shape memory alloys. Materials properties handbook titanium alloys. ASM International. Materials Park, Ohio, pp. 1035–1048.

Duffy, J., Campbell, J.D., Hawley, R.H., 1971. On the use of torsional Hopkinson bar to study rate effects in 1100-0 aluminum. Journal of Applied Mechanics 38, 83–91.

Follansbee, P.S., 1985. The Hopkinson bar. Mechanical Testing, Metals Handbook, ninth ed. American Society for Metals, Materials Park, Ohio, pp. 198–217.

Gray, G.T., Blumenthal, W.R., Trujillo, C.P., Carpenter, R.W., 1997. Influence of temperature and strain rate on the mechanical behavior of Adiprene L-100. Journal de Physique IV Colloq. C3 (DYMAT 97) 7, 523–528.

James, R.D., Hane, K.F., 2000. Martensitic transformations and shape-memory materials. Acta Materialia 48, 197–222.

Kolsky, H., 1949. An investigation of mechanical properties of materials at very high rates of loading. Proceedings of the Physics Society of London B 62, 676–700.

Lindholm, U.S., 1964. Some experiments with the split Hopkinson pressure bar. Journal of the Mechanics and Physics of Solids 12, 317–335.

Meyers, M.A., 1994. Dynamic behavior of materials. Wiley-Interscience, New York, pp. 305–310.

Nemat-Nasser, S., Isaacs, J.B., Starrett, J.E., 1991. Hopkinson techniques for dynamic recovery experiments. Proceedings of the Royal Society of London A 435, 371–391.

Ravichandran, G., Chen, W., 1991. Dynamic behavior of brittle materials under uniaxial compression. In: K.S. Kim (Ed.) Experiments in Micromechanics of Fracture Resistant Materials. AMD-130, ASME, New York, pp. 85–90.

Ravichandran, G., Subhash, G., 1994. Critical appraisal of limiting strain rates for compression testing of ceramics in a split Hopkinson pressure bar. Journal of the American Ceramic Society 77, 263–267.

Schetky, L.M., Perkins, J., 1978. The 'quiet' alloys. Machine Design (April 6), 202–206.

Stoeckel, D., Yu, W., 1991. Superelastic Ni–Ti wire. Wire Journal International (March), 45–50.

Togami, T.C., Baker, W.E., Forrestal, M.J., 1996. A split Hopkinson bar technique to evaluate the performance of accelerometers. Transactions of the ASME, Journal of Applied Mechanics 63, 353–356.

Wayman, C.M., 1993. Shape memory alloys. MRS Bulletin (April), 49–56.

Wu, X.J., Gorham, D.A., 1997. Stress equilibrium in the split Hopkinson pressure bar test. Journal de Physique IV Colloq. C3 (DYMAT 97) 7, 91–96.